REPORT DOCUMENTATION PAGE

Form Approved
OMB No. 0704-0188

1. AGENCY USE ONLY (Leave blank)	2. REPORT DATE	3. REPORT TYPE AND DATES COVERED
	2/16/96	Final 5/22/92-8/21/95

4. TITLE AND SUBTITLE

"Excitonic Nonlinear Optical Properties in Quantum Wires and Prismatic Quantum Dots"

5. FUNDING NUMBERS

~~AFOSR Contract No.~~
~~F49620-92-J-~~0382

61102F
2305/FS

6. AUTHOR(S)

Frank L. Madarasz

7. PERFORMING ORGANIZATION NAME(S) AND ADDRESS(ES)

Center for Applied Optics
University of Alabama in Huntsville
Huntsville, AL 35899

8. PERFORMING ORGANIZATION REPORT

AFOSR-TR-96

G108

9. SPONSORING/MONITORING AGENCY NAME(S) AND ADDRESS(ES)

Air Force Office of Scientific Research -NE
Bolling AFB
Washington, D.C.

AGENCY REPORT NUMBER

AFOSR Contract No.
F49620-92-J-0382

11. SUPPLEMENTARY NOTES

12a. DISTRIBUTION/AVAILABILITY STATEMENT

Approved for public release;
distribution unlimited.

12b. DISTRIBUTION CODE

19960320 045

13. ABSTRACT *(Maximum 200 words)*

Exciton and biexciton binding energies, and wave functions are calculated with a three parameter variational model in an effective mass approximation for a rectangular GaAs quantum well wire surrounded by an AlGaAs cladding. Moreover, the Al interdiffusion into the wire and the finite band offsets between the wire and the cladding have been included. For the range of dimensions studied, the inclusion of the Al interdiffusion had a pronounced affect on the binding energies when compared to those obtained from the infinite barrier model. In particular, for small (symmetric) wire dimensions the binding energies remain finite. And for asymmetric wires all binding energies were markedly lowered. Using the results of the exciton and biexciton calculation, the third-order nonlinear optical susceptibility was calculated as a function of pump-probe frequencies in a small range about the exciton absorption resonance. The calculation was restriced to the optical nonlinearity via the biexciton state arising from the population saturation of the exciton state. It was found, depending upon wire dimensions, broadening parameter(s) size, and the amount of pump detuning, values of the imaginary parts of the susceptibilities to be on the order of -10^{-2} to -10^{-1} esu and a fairly large off-resonance absorption due to biexciton formation.

14. SUBJECT TERMS	15. NUMBER OF PAGES
Quantum Wires, Excitons, Biexcitons, Nonlinear Optical Susceptibilities	9
	16. PRICE CODE

17. SECURITY CLASSIFICATION OF REPORT	18. SECURITY CLASSIFICATION OF THIS PAGE	19. SECURITY CLASSIFICATION OF ABSTRACT	20. LIMITATION OF ABSTRACT
			UL

Summary

Quantum confined structures--wells, wires, and dots (potential energy well confinement, on an atomic scale (10-200 angstroms), in one-, two-, or three-dimensions)--exhibit a rich variety of enhanced electronic and optical properties relative to bulk materials. In general, they posses strong optical nonlinearities, very high third-order optical suseptibilities, $\chi^{(3)}$, which may be profitably employed in performing a myriad of opto-electronic functions. In particular, exciton based devices show great promise in application to optical information processing. The underlying reason is based on the two following properties: First, exciton binding energies are enhanced by quantum confinement to values more than 10 meV--this allows exciton transitions to be well separated from the band-to-band transitions and also allows the transitions to persist even at room temperature. The excitonic peaks can be modulated by external perturbations such as an electric field leading to the quantum confined Stark effect or magnetic field, which can be exploited for optical modulators, switching devices, memories, and a host of other opto-electronic applications.

Unfortunately, direct measurement of $\chi^{(3)}$ values in quantum confined structures is difficult. Estimates are usually inferred from other optical measurements or some combination of such measurements as photoluminescence, absorption, and transmission spectra. In addition, it is difficult to experimentally tailor the nonlinear optical response because of the number of physical parameters involved and of the indirectness with which the optical nonlinearities are determined. The need for a theoretical model to provide guidelines for the optimization of the nonlinear response is imperative; one which is physically motivated by the properties of the material and structure and will a priori determine the relevant parameters and thus reduce considerably a costly and time consuming experimental effort.

The model developed on AFOSR Contract No. F49620-92-J-0382, and qualitatively described in the abstract, is a major step in this direction and has so been recognized in the literature. The quantitative aspects of theory are given in great detail and can be found in the peer reviewed journal articles cited in this report. However, for completeness of the report I have included, in both graphical and tabulated form, the significant results of the research.

In Tables I and II I compare the exciton and biexciton binding energies when calculated with finite band offset potentials and with infinite potentials in a rectangular, $L \neq W$, wire. Table I features the holding of L, the strong confinement dimension, fixed and the varying of W, the dimension of the finite band offset potentials. On the other hand, Table II holds W fixed and varies L. In each table, the varied dimension $\geq$ the fixed dimension. The binding energy percent

difference is simply: % diff.=|finite-infinite|/finite. The general trend in either table is obvious: the larger the dimensions the smaller the percent difference.

Another general observation, between the two tables, is that for any set of dimensions, LxW, larger (one or both) or equal to 50x50 $Å^2$ the corresponding percent differences are comparable to within a few tenths. The implication is clear--while wave function penetration is important in lowering the binding energy it is not significant enough, at least for ground state energies, to affect the results whether L<W or L>W. Conversely, for any set of dimensions in which one (or both) is smaller than or equal to 25 Å the corresponding percent differences are not comparable. Here, L<W results in a significant difference between the binding energies than when L>W within the set. Finally, it appears that for the larger dimensions, nominally 400 Å and above, wave function penetration is insignificant, at least for the ground state energies, and the infinite potential model may be used in both confinement directions.

With reference to Table III, first note that the inclusion of finite band offsets lowers both electron and hole single particle subband energies for the narrowest grading (almost abrupt), W/16, giving approximately 61% difference for the electron and 35% difference for the hole. And, of course this is precisely what is expected to happen. Fixing our attention on just the electron states for the moment, it can be seen that, by increasing the diffusion length from W/16 to W/8 and then from W/8 to W/4, the subband energies rise. The reason for this trend is clear especially when considering the graded well structure: as the diffusion width is increased the bottom of the well narrows pushing the states up. However, when increasing the diffusion length from W/4 to W/2 the trend appears to be reversed. The cause of this reversal is also clear: the well is now "over graded". That is, under this condition, there is enough Al concentration located at the center of the well to change the fundamental gap from that of pure GaAs to some percentage AlGaAs--the gap is increased and the well, as it rises, begins to flatten out. Relative to the bottom of the graded well the subband energy has indeed become smaller, but relative to the bottom of the GaAs well has continued to rise. In fact, as the fraction of Al in the center of the graded well, approaches x=0.3 the subband(s) coalesces at the bottom of the well and form the conduction band in bulk AlGaAs; the lowering of subband energies is to be expected.

A similar argument can be made for the hole subband energies. However, it is apparent from Table IV that, when the diffusion length reaches W/4 the subband energy exceeds that of the infinite barrier model. The cause of such a result is not totally unexpected. The barrier height for the holes is two thirds of that for the electrons. This means that the corresponding Al-grading of the valence band produces a well which is narrower for z<W/2 and wider for z>W/2 than that of

the conduction band. One then expects a larger percentage increase in energy for the lower-lying hole subbands bands. For example, changing the diffusion length from W/8 to W/4 produces about a 19% increase in the electron subband energy and about a 34% increase in the hole subband energy.

The exciton and biexciton binding energies are lowered with the inclusion of the finite band offsets by approximately 14% for the smallest diffusion length of W/16. The evolution of their respective values with increasing Al-grading width can easily be explained in terms of the arguments given above for the electron and hole subbands. Similarly, the exciton and biexciton ground state energies are lowered with the inclusion of the finite band offsets. Since each is dominated by the fundamental band gap energy, their change is rather small, both being approximately 4% for the smallest diffusion length of W/16. Because of such a small change in the exciton ground state energy, the effect on the magnitude of optical susceptibility is negligible. However, at higher densities of excitons and biexcitons than considered here, the lower binding energies do affect the stability of the system and will thus limit the operational conditions under which peak $\chi^{(3)}$ values may be obtained and maintained.

The third-order nonlinear optical susceptibility, Im $\chi^{(3)}$, Fig. 1-4, was calculated as a function of pump-probe frequencies in a small range about the exciton absorption resonance. The negative peak in all of these spectra indicates transmission and is due to a bleaching (saturation) of the one-pair exciton transition. Physically, the initial exciton population created by the pump beam tends to amplify the probe beam, by way of stimulated emission, when the probe energy is tuned at or near the exciton linear absorption peak. Depending upon wire dimensions and the amount of pump detuning, values of the susceptibilities on the order of -10^{-1} to -10^{-2} esu were found.

Another feature in all of the curves is the non linear optical absorption--the region of positve Im $\chi^{(3)}$. The absorption may be attributed to the formation of the excitonic molecule[17-19]. The initial exciton population enables the probe to be more strongly absorbed when its energy matches the exciton-biexciton transition energy.

TABLE I Exciton/biexciton binding energies (E_B^X /E_B^{XX}) in GaAs/$Al_{0.3}Ga_{0.7}As$ quantum wires of various dimension, L≤W, with and without finite band offset potentials included.

Wire Dimensions		Exciton Binding Energy (meV)		% Diff.	Biexciton Binding Energy (meV)		% Diff.
L (Å)	W (Å)	Finite	Infinite		Finite	Infinite	
10	10	21.78	47.56	118.4	15.15	33.32	119.9
10	25	23.58	36.84	56.2	16.36	25.55	56.2
10	50	20.89	28.15	34.8	14.50	19.48	34.3
10	75	18.38	23.40	27.3	12.78	16.22	26.9
10	100	16.51	20.25	22.7	11.51	13.96	21.4
10	125	15.08	18.11	20.1	10.54	12.61	19.7
10	150	13.90	16.43	18.2	9.73	11.46	17.8
25	25	21.38	30.96	44.8	14.64	21.29	45.4
25	50	19.27	25.06	30.1	13.19	17.19	30.3
25	75	17.17	21.42	24.8	11.75	14.66	24.8
25	100	15.55	18.89	21.5	10.64	12.93	21.6
25	125	14.29	17.00	18.9	9.78	11.62	18.9
25	150	13.23	15.52	17.3	9.05	10.61	17.2
50	50	17.10	21.39	25.1	11.45	14.64	27.9
50	75	15.49	18.85	21.7	10.58	12.88	21.8
50	100	14.20	16.95	19.4	9.690	11.58	19.5
50	125	13.16	15.47	17.5	8.984	10.57	17.7
50	150	12.26	14.27	16.4	8.373	9.755	16.5
75	75	14.17	16.93	19.5	9.664	11.57	19.7
75	100	13.10	15.44	17.8	8.935	10.54	18.0
75	125	12.23	14.23	16.4	8.343	9.707	16.4
75	150	11.47	13.24	15.5	7.820	9.030	15.5
100	100	12.20	14.22	16.6	8.313	9.710	16.8
100	125	11.45	13.22	15.4	7.806	9.023	15.6
100	150	10.78	12.37	14.8	7.352	8.447	14.9
125	125	10.78	12.37	14.7	7.348	8.440	14.9
125	150	10.19	11.64	14.2	6.948	7.931	14.1
150	150	9.678	11.00	13.6	6.595	7.506	13.8
200	200	8.091	9.091	12.4	5.516	6.207	12.5
250	250	7.008	7.807	11.4	4.781	5.335	11.6
300	300	6.168	6.874	11.5	4.211	4.702	11.7

TABLE II Exciton/biexciton binding energies (E_B^x /E_B^{xx}) in GaAs/$Al_{0.3}Ga_{0.7}As$ quantum wires of various dimension, L≥W, with and without finite band offset potentials included.

Wire Dimensions		Exciton Binding Energy (meV)		% Diff.	Biexciton Binding Energy (meV)		% Diff.
L (Å)	W (Å)	Finite	Infinite		Finite	Infinite	
10	10	21.78	47.56	118.4	15.15	33.32	119.9
25	10	19.87	36.84	85.4	13.61	25.55	87.7
50	10	17.46	28.15	61.2	11.93	19.48	63.2
75	10	15.69	23.40	49.1	10.71	16.22	51.4
100	10	14.32	20.25	41.4	9.775	13.96	42.9
125	10	13.23	18.11	36.9	9.022	12.61	39.7
150	10	12.32	16.43	33.4	8.402	11.46	36.4
25	25	21.38	30.96	44.8	14.64	21.29	45.4
50	25	18.61	25.06	34.7	12.72	17.19	35.1
75	25	16.61	21.42	29.0	11.34	14.66	29.3
100	25	15.08	18.89	25.3	10.29	12.93	25.7
125	25	13.86	17.00	22.7	9.454	11.62	23.0
150	25	12.86	15.52	20.7	8.772	10.61	21.0
50	50	17.10	21.39	25.1	11.45	14.64	27.9
75	50	15.46	18.85	21.9	10.55	12.88	22.2
100	50	14.16	16.95	19.7	9.659	11.58	19.9
125	50	13.11	15.47	18.0	8.937	10.57	18.3
150	50	12.23	14.27	16.7	8.338	9.755	17.0
75	75	14.17	16.93	19.5	9.664	11.57	19.7
100	75	13.10	15.44	17.9	8.928	10.54	18.1
125	75	12.20	14.23	16.6	8.318	9.707	16.7
150	75	11.45	13.24	15.7	7.803	9.030	15.7
100	100	12.20	14.22	16.6	8.313	9.710	16.8
125	100	11.43	13.22	15.7	7.789	9.023	15.8
150	100	10.77	12.37	14.9	7.341	8.447	15.1
125	125	10.78	12.37	14.7	7.348	8.440	14.9
150	125	10.20	11.64	14.1	6.952	7.931	14.1
150	150	9.678	11.00	13.6	6.595	7.506	13.8
200	200	8.091	9.091	12.4	5.516	6.207	12.5
250	250	7.008	7.807	11.4	4.781	5.335	11.6
300	300	6.168	6.874	11.5	4.211	4.702	11.7

TABLE III

Infinite Potential Results

vs.

Finite Graded Potential Results

(GaAs Wire -- $Al_{0.3}Ga_{0.7}As$ Cladding)[a]

L x W = 125 x 75 Å

	Infinite	W/16*	W/8*	W/4*	W/2*
$\mathcal{E}_1^e$(meV)	99.75	38.67	41.69	51.38	47.24
$\mathcal{E}_1^h$(meV)	14.85	9.66	11.11	16.73	16.76
$\eta_x(a_o)$	362.20	395.45	393.58	389.95	395.12
E_B^X(meV)	-14.23	-12.27	-12.35	-12.54	-12.29
V_{eh}(meV)	-19.69	-16.85	-16.97	-17.25	-16.88
E_{go}^X(eV)	1.662	1.597	1.602	1.617	1.668
$\xi(a_o)$	1024.43	1116.79	1111.62	1101.55	1115.88
$\eta_{xx}(a_o)$	293.38	320.36	318.86	313.96	318.09
E_B^{XX}(meV)	-9.71	-8.36	-8.42	-8.55	-8.38
V^{XX}(meV)	-53.61	-45.88	-46.22	-46.97	-45.97
E_{go}^{XX}(eV)	3.31	3.186	3.195	3.225	3.328
$z(0.01\,u_{e\,max}^{(1)})$ (Å)		97.00	99.00	100.00	115.00
$z(0.01\,u_{h\,max}^{(1)})$ (Å)		61.00	62.00	63.00	69.00

a. Band Offsets--0.6 Conduction, 0.4 Valence

* 1/2 Al Grading Width

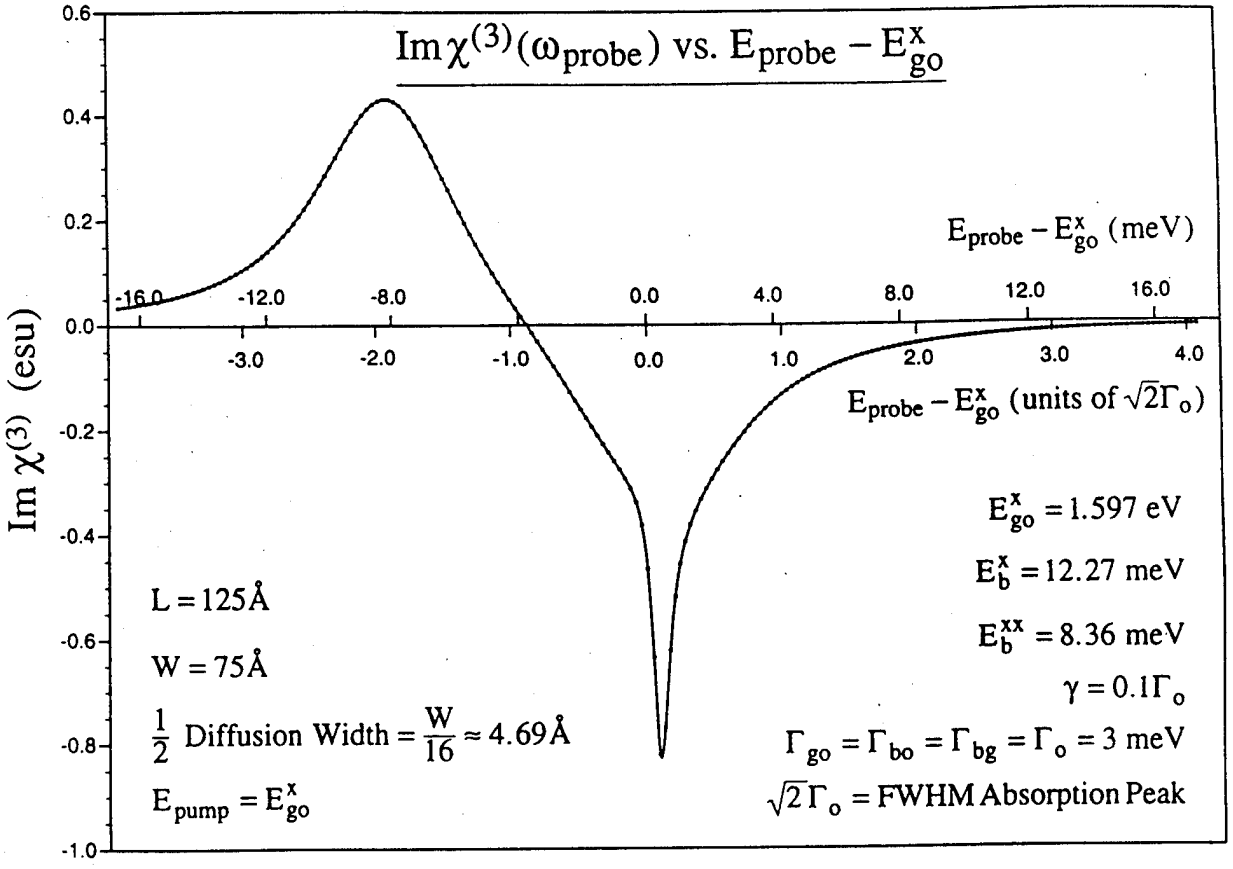

FIG. 1 The imaginary part of the third-order optical susceptibility as a function of the probe energy, E_{probe}, for a dual beam pump-probe experiment. The pump is set at exciton resonance and the longitudinal broadening parameter, γ, is one-tenth the value of the transverse broadening parameters, Γ_{ij}. E^{x}_{go} is the ground state energy of the exciton, and E^{x}_{b} and E^{xx}_{b} are the binding energies of the exciton and biexcitons respectively.

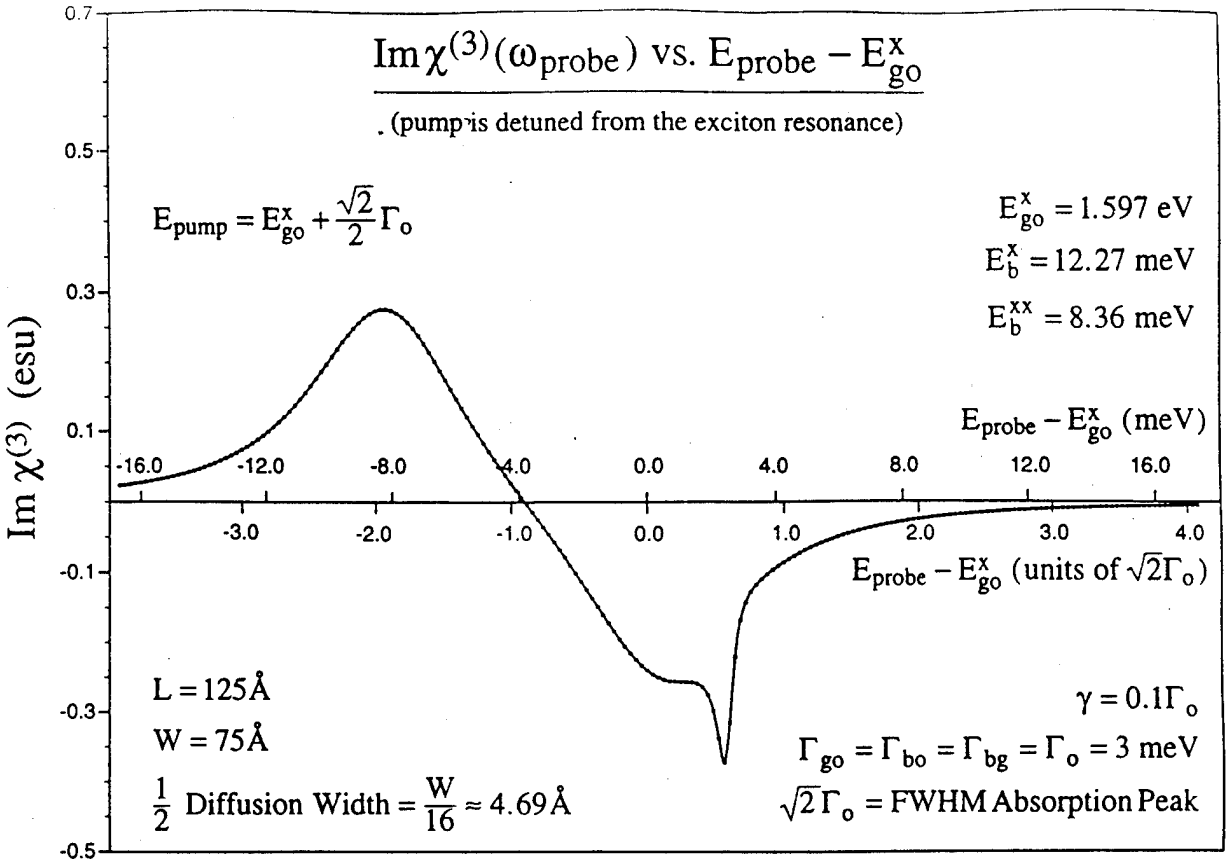

FIG. 2 Same as figure 1 but with the pump detuned slightly above the exciton resonance.

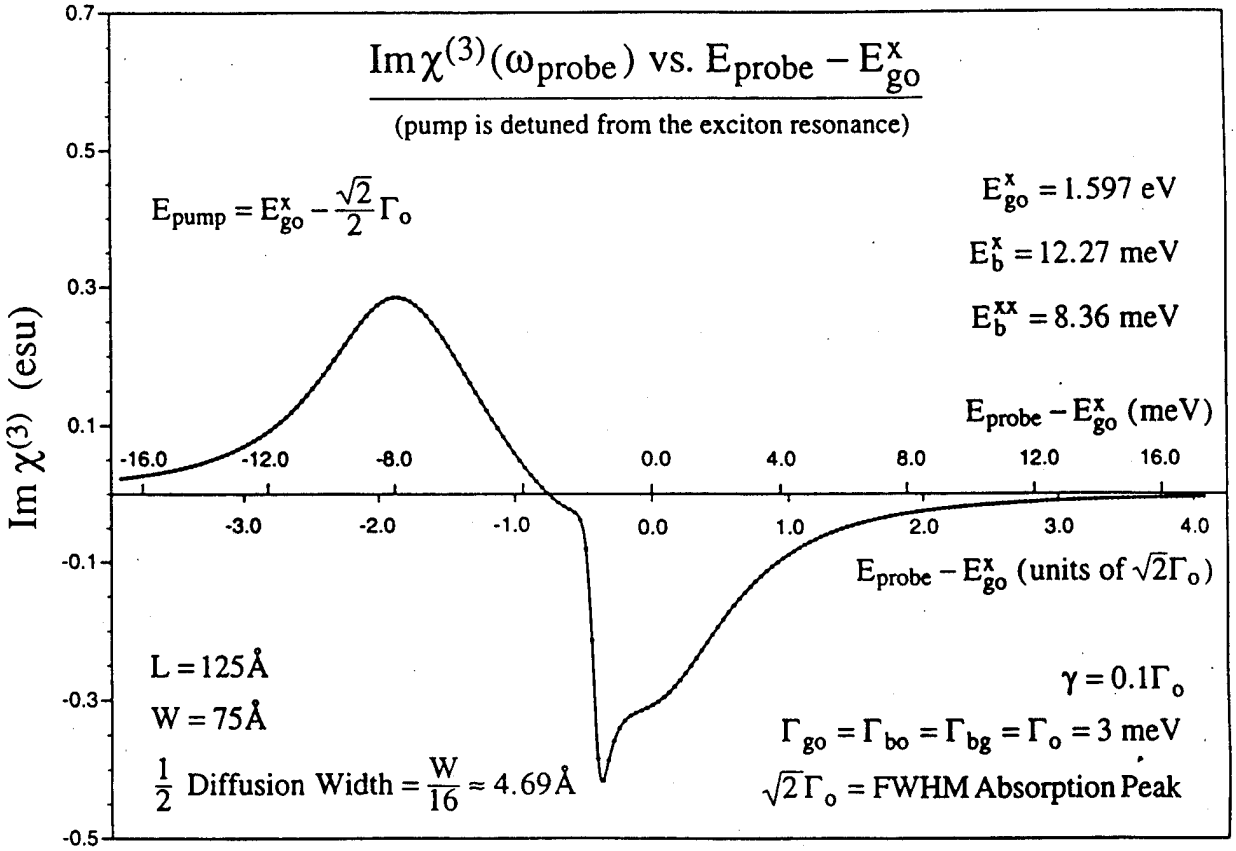

FIG. 3 Same as figure 1 but with the pump detuned slightly below the exciton resonance.

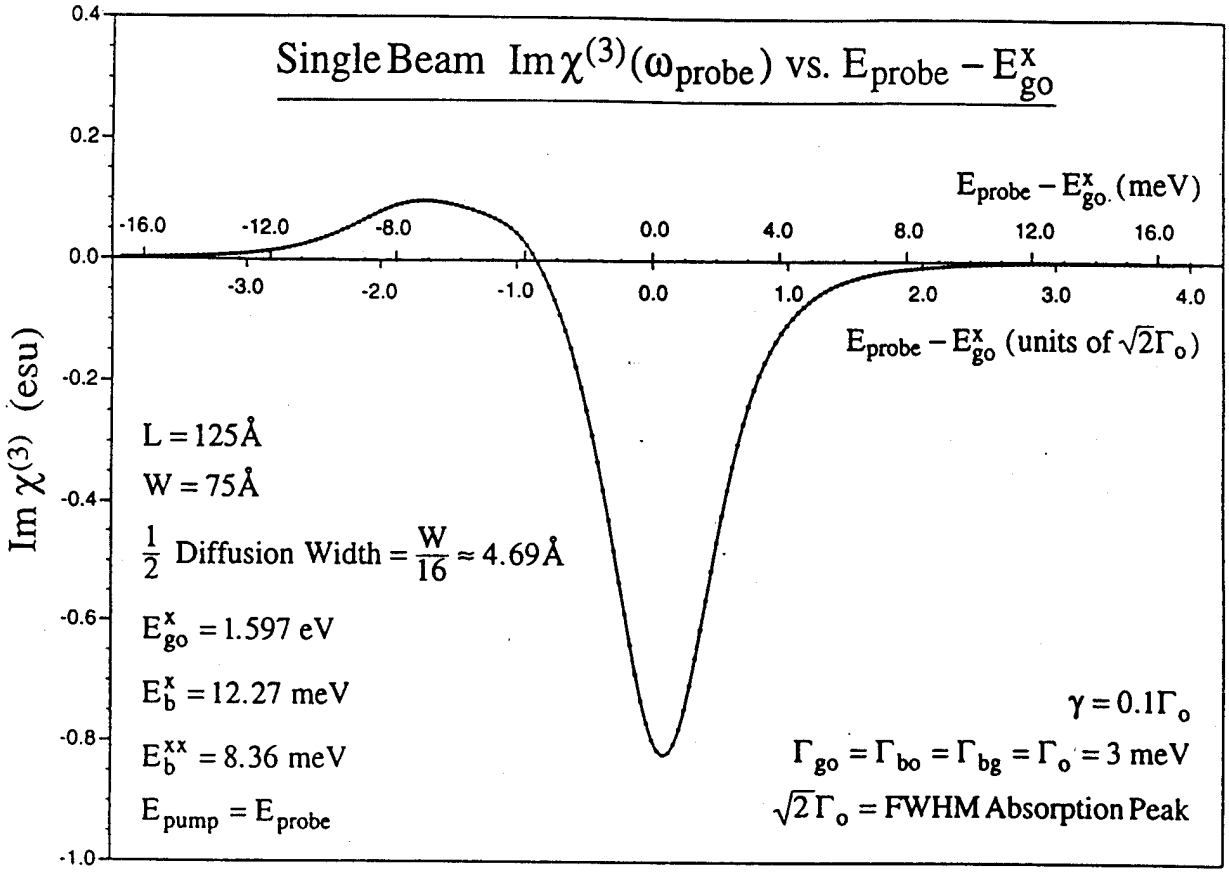

FIG. 4 Imaginary part of the third-order optical susceptibility as a function of the energy for a single beam pump-probe experiment. The longitudinal broadening parameter is one-tenth the value of the transverse broadening parameters.